Two-dimensional turbulence above topography

By FRANCIS P. BRETHERTON

National Center for Atmospheric Research, P.O. Box 3000, Boulder, Colorado 80303

AND DALE B. HAIDVOGEL

Massachusetts Institute of Technology, Cambridge†

In a turbulent two-dimensional flow enstrophy systematically cascades to very small scales, at which it is dissipated. The kinetic energy, on the other hand, remains at large scales and the total kinetic energy is constant. Above random topography an initially turbulent flow tends to a steady state with streamlines parallel to contours of constant depth, anticyclonic around a bump. A numerical experiment verifies this prediction. In a closed basin on a beta-plane the solution with minimum enstrophy implies a westward flow in the interior, returning in narrow boundary layers to the north and south. This result is interpreted using a parameterization of the effects of the eddies on the large-scale flow. The numerical solution is in qualitative agreement, but corresponds to a minimum of a more complex measure of the total enstrophy than the usual quadratic integral.

1. Introduction

This note considers two-dimensional turbulence in a homogeneous layer of almost inviscid liquid in a thin quasi-planar shell of irregular thickness, the whole system rotating rapidly about the normal axis. If the Rossby number for the flow and the fractional change in layer thickness are both small compared with unity, and if dissipation is temporarily neglected, the dimensionless equation of motion may be written as

$$D\{\nabla^2\psi + h(x, y)\}/Dt = 0, \tag{1}$$

where

$$\frac{D}{Dt} = \frac{\partial}{\partial t} - \frac{\partial\psi}{\partial y}\frac{\partial}{\partial x} + \frac{\partial\psi}{\partial x}\frac{\partial}{\partial y} \tag{2}$$

is the material derivative following a fluid particle with the non-divergent flow

$$u = -\partial\psi/\partial y, \quad v = \partial\psi/\partial x, \tag{3}$$

and $h(x, y)$ is the local fractional change in layer thickness divided by the Rossby number, hereafter called the 'topography'. Equation (1) then states that the potential vorticity

$$q = \nabla^2\psi + h \tag{4}$$

is constant on a fluid particle, and implies that for suitable lateral boundary conditions the total enstrophy

$$Q = \tfrac{1}{2}\int(\nabla^2\psi + h)^2\,dx\,dy \tag{5}$$

and energy

$$E = \tfrac{1}{2}\int(\nabla\psi)^2\,dx\,dy \tag{6}$$

† Present address: Center for Earth and Planetary Physics, Pierce Hall, Harvard University, Cambridge, Massachusetts 02138.

9

are invariant with time. Except for the inclusion of the 'topographic' term h these equations are identical with those of conventional two-dimensional turbulence.

The motivation for this study came from the recently discovered mesoscale eddies in the deep ocean, but this application will be elaborated elsewhere. Meanwhile the time evolution of an initially random flow described by (1) may be regarded as an interesting fluid-dynamical problem in its own right. It will be seen that the topographic term dramatically changes the character of the non-linear development of the turbulent spectrum.

Although most of the principles are valid for quite general topography, the discussion is orientated around the assumption that $h(x,y)$ has the qualitative character implied by an isotropic spectrum proportional to κ^{-2}, where κ is the total wavenumber. This spectral shape approximates that of irregularities on the floor of the ocean in many areas (Bell 1975). The mean-square slope $S^2 = \overline{|\nabla h|^2}$ is then formally infinite, but when, as in practice, contributions to it are cut off at a maximum wavenumber κ_0 it has a finite value

$$S_0^2 \propto \kappa_0, \tag{7}$$

i.e. the one-dimensional slope spectrum is white.

We shall introduce later an additional constant large-scale slope described by

$$h = \beta y, \tag{8}$$

simulating the variation of the Coriolis parameter with latitude, which is so important in geophysical fluid dynamics. The random topography will then be seen to be crucially important in effecting transfers between the large-scale potential-vorticity field βy and the enstrophy associated with the eddies themselves. It will also be shown to be associated with the generation of large-scale circulations.

2. The enstrophy cascade

The evolution of a turbulent flow field described by (1) with $h \equiv 0$ is well understood in qualitative terms (Batchelor 1969). If U is a typical particle velocity and L the dominant length scale of the eddies, U is approximately constant but L increases with time as small eddies coalesce to form larger ones at a rate comparable to U/L. Kinetic energy is thus systematically transferred to smaller wavenumbers (an inverse cascade) while enstrophy is cascading to larger wavenumbers.

The deep-seated character of this process may be seen by considering a moving circuit C of fluid particles (figure 1) each with the same vorticity q (Batchelor 1969). An inherent property of turbulent motion is that neighbouring fluid particles tend, on the average, to separate systematically, so the length l of such a circuit increases approximately exponentially with time. Since the area enclosed by C is constant it becomes more and more convoluted, with a finer and finer structure. This is the cascade of q to high wavenumbers, a kinematic property of the turbulence which continues until viscosity (however small)
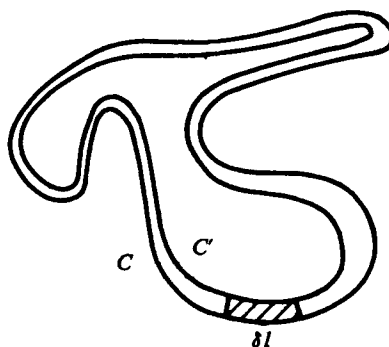
FIGURE 1. Two neighbouring circuits C and C' of material particles being deformed and stretched in a turbulent flow field. The potential vorticity q is constant around C, and has the value $q + \delta q$ around C'.

ultimately dissipates the fluctuations on some suitably small scale. Thus the total enstrophy

$$Q = \tfrac{1}{2} \int q^2 \, dx \, dy \qquad (9)$$

must in practice decrease with time, at a rate set primarily by the larger energy-containing scales of motion, which contribute to the strain field, and essentially independent of whatever small-scale dissipative mechanism is invoked.

Kinetic energy, on the other hand, is not tied to specific particles, and this argument does not apply. Indeed, because the enstrophy associated with a Fourier component of wavenumber κ is $\kappa^2 E(\kappa)$, where $E(\kappa)$ is the energy, a small-scale dissipative process will reduce the total enstrophy much faster than the energy, and in the limit of infinitely large κ, at which all such dissipation takes place, the total energy E must remain effectively constant. Thus we are led to conclude that

$$Q = \sum_{\kappa} \kappa^2 E(\kappa) \qquad (10)$$

decreases, whereas

$$E = \sum_{\kappa} E(\kappa) \qquad (11)$$

is constant, which can occur only if $E(\kappa)$ becomes concentrated more and more at smaller values of κ. Hence the inverse energy cascade.

It is worth noting some of the subtleties of this argument. There is an implicit assumption that the vorticity q is dynamically sufficiently passive that the particular line elements lying in a contour of constant q are not exceptions to the general rule that time elements tend to grow in a random strain field. This assumption is plausible if the local rate of strain is dominated by contributions from a wide range of scales, but the very existence of complicated *steady* flows in which contours of q and ψ coincide shows that such exceptions can exist. The indefinite extension of such circuits C is, however, a definitive indicator of the cascade. For consider a neighbouring circuit C' consisting of particles of vorticity $q + \delta q$, where δq is infinitesimal. The area of the band between C and C' is constant, so as the length l of either increases the average separation between them must become less, i.e. $|\nabla q|^2$ must tend to infinity, and dissipation must cause a definite decrease in the magnitude of Q. The extent of the reduction in total enstrophy clearly

depends on the proportion of the fluid elements which are subject to such drastic strain. The numerical experiments of Herring *et al.* (1974) demonstrate convincingly that for conventional two-dimensional turbulence the cascade is indeed a rapid and dominant effect.

3. A minimum-enstrophy principle

Now consider a similar argument when the topographic term is present. The potential vorticity q is still constant on fluid particles, and in the absence of dissipation Q and E, defined by (5) and (6), are invariants. However if there is a cascade, as defined by the indefinite extension of a significant fraction of the contours of constant q, the enstrophy Q must decrease with time. It thus becomes meaningful to ask: what is the flow pattern which minimizes Q for a given E? We shall treat this first for the simplest boundary conditions, in which both $h(x, y)$ and $\psi(x, y)$ are assumed to be periodic in x and y with some large period X. Having found the minimal flow pattern, we shall then discuss its relevance to turbulent development.

The first problem is a simple exercise in the calculus of variations. We require

$$\delta Q + \mu \delta E = \int (\nabla^2 \psi + h)\, \delta(\nabla^2 \psi)\, dx\, dy + \mu \int \nabla \psi \cdot \nabla\, \delta \psi\, dx\, dy \qquad (12)$$
$$= \int \nabla^2 \{\nabla^2 \psi + h - \mu \psi\}\, \delta \psi\, dx\, dy$$

to vanish for all infinitesimal variations $\delta \psi$ which are also periodic with period X. The parameter μ is a Lagrange multiplier, a constant to be determined later. Using the periodicity to eliminate the outer ∇^2, we infer a *necessary* condition

$$\nabla^2 \psi + h = \mu \psi. \qquad (13)$$

This is easily solved in terms of Fourier transforms. If

$$h(x, y) = \sum_{k, l} \hat{h} \exp[i(kx + ly)]$$

then
$$\hat{\psi} = \hat{h}/(\mu + \kappa^2), \qquad (14)$$

where $\kappa^2 = k^2 + l^2$.

Equation (14) shows that there is indeed a unique stationary solution ψ_0 for each value of the constant μ. μ defines a length scale

$$L_0 = \mu^{-\frac{1}{2}} \qquad (15)$$

such that on scales small compared with L_0

$$q = \nabla^2 \psi_0 + h \sim 0. \qquad (16)$$

This is consistent with fluid particles being swept completely over small-scale bumps, the associated contraction of vortex lines implying anticyclonic vorticity in regions where the shell is relatively thin. However, on scales large compared with L_0

$$\psi_0 \sim \mu^{-1} h, \qquad (17)$$

so that the flow is along contours of constant $h(x, y)$. Since the κ^2 term in (14) diminishes the magnitude of $\hat{\psi}$ below the value $\mu^{-1} \hat{h}$, the overall flow pattern

$\psi_0(x, y)$ can be characterized as similar to $h(x, y)$ but with scales smaller than L_0 smoothed out.

To determine L_0, note that the mean-square particle speed is

$$U^2 = \overline{|\nabla \psi_0|^2} = \sum_\kappa \frac{\kappa^2 |\hat{h}|^2}{(\kappa^2 + \mu)^2} \tag{18}$$

$$\sim \frac{1}{\mu^2} \sum_{k=0}^{\mu^{-\frac{1}{2}}} \kappa^2 |\hat{h}|^2 = \frac{1}{\mu^2} S_0^2, \tag{19}$$

where S_0 is the root-mean-square 'slope' smoothed to exclude wavenumbers greater than $\mu^{\frac{1}{2}} = L_0^{-\frac{1}{2}}$. Because of the non-dimensionalization in (1), S_0 is the true slope times the ratio of horizontal to vertical scales, divided by the Rossby number. Thus, for a given energy level E equation (18) may be solved for μ. For the preferred topography in which the one-dimensional spectral density is proportional to κ^{-2},

$$L_0 \propto U^{\frac{2}{3}}. \tag{20}$$

In any case μ has to be positive, otherwise contributions in (18) from wavenumbers near $\kappa^2 = -\mu$ would imply an effectively infinite kinetic energy density. Thus the flow is not only approximately around contours of constant h, but also has a definite sign: anticyclonic (clockwise) circulation around a bump, cyclonic around a hollow.

We see therefore that for each total energy E there is a unique flow field $\psi_0(x, y)$ for which Q is stationary to small variations. It is readily demonstrated that for positive μ this is in fact a minimum. Such a flow field is also stationary in *time*, because the potential vorticity q is constant along contours of constant ψ. This is no accident, as may be seen from the following argument. Suppose ψ_0 were to develop in time to a different field ψ'. In an inviscid flow the total enstrophy and energy would be constant, i.e. they would have to equal those for ψ_0. But it has just been demonstrated that the *only* field ψ' with this enstrophy and energy is ψ_0. Hence no development can occur.

4. The development of turbulent flows

How is this minimum-enstrophy solution relevant? We have seen how the random but systematic stretching of time elements in a turbulent flow implies an enstrophy cascade. So long as this persists Q must decrease. Yet Q is bounded below by the value Q_0 appropriate to the overall energy level E and the topography $h(x, y)$. Thus the flow must tend towards some state in which the cascade is halted, i.e. a steady state in which

$$q \equiv \nabla^2 \psi + h = F(\psi), \tag{21}$$

where F is some possibly nonlinear function which is single valued at least along each closed streamline. It will be seen later that in practice this does usually occur, and furthermore F is nearly linear. Then $\psi_0(x, y)$ as given by (13) and (18) is a good approximation to the final flow pattern, though by no means a perfect one. The time scale for this transformation seems to be a multiple of L_0/U. Thus the minimum-enstrophy principle appears to provide a useful framework for discussing the evolution of an initially turbulent flow above topography.

However, we shall show in the appendix that in fact there are many alternative formulations of this principle, each one designating an absolutely stable steady state corresponding to a different monotonically increasing function F in (21). In any given realization only one of these measures is actually minimized, each of the others tending to a constant value larger than its minimum. Which ultimate steady state is selected must depend in some presently unknown way on the initial conditions. For some initial states the flow described by (13) is certainly inaccessible, even though the total energy may correspond. These tantalizing considerations in no way negate the remaining conclusions of this paper, but do show that all is not well understood. Nevertheless, the overwhelming conclusion remains that, given a continuing enstrophy cascade at approximately constant total energy, the turbulence must evolve into a steady state in which the flow on the larger scales is along contours of constant h, with h increasing to the right. A similar tendency for the flow to follow contours, but not the steady state, was noted by Holloway & Hendershott (1974).

5. The role of saddle points

Before discussing the experiment designed to test these arguments, three points need clarification: the nature of the cascade when the flow is near ψ_0, the precise role of viscosity and the influence of boundaries. If we set

$$\psi = \psi_0 + \phi \tag{22}$$

and linearize in ϕ, (1) becomes

$$\partial(\nabla^2\phi)/\partial t + J(\psi_0, \nabla^2\phi) - \mu J(\psi_0, \phi) = 0, \tag{23}$$

where J is the Jacobian operator. The first two terms describe the advection of vorticity by the flow ψ_0, the last term the production of perturbation vorticity by flow across the contours of constant q_0. The qualitative nature of the motion depends on whether the scale L of the perturbation is large or small compared with L_0. If it is large, the last term dominates, and we have essentially topographic Rossby waves with phase speed much greater than U. If, on the other hand, $L \ll L_0$ the perturbation vorticity is advected by the flow field ψ_0.

Of particular interest are the neighbourhoods of saddle points of $\psi_0(x, y)$. It is well known that in such persistent deformation fields gradients of a passive advected scalar are greatly amplified as sinusoidal variations are aligned parallel to the outflow axis and compressed in the perpendicular direction. It is less obvious that such saddle points are also traps for topographic Rossby waves. If

$$\psi_0 = ax^2 - by^2 \tag{24}$$

equation (23) becomes

$$\frac{\partial}{\partial t}\nabla^2\phi + \left(by\frac{\partial}{\partial x} + ax\frac{\partial}{\partial y}\right)(\nabla^2\phi - \mu\phi) = 0. \tag{25}$$

This has solutions of the form

$$\phi = \mathscr{R}[\hat{\phi}(t) \exp i\{k(t)x + l(t)y\}] \tag{26}$$

if

$$d\{(k^2 + l^2)\hat{\phi}\}/dt = 0 \tag{27}$$

and

$$\frac{\kappa^2 + l^2}{\kappa^2 + l^2 + \mu}\frac{dk}{dt} + bl = 0, \quad \frac{\kappa^2 + l^2}{\kappa^2 + l^2 + \mu}\frac{dl}{dt} + ak = 0. \tag{28}$$

These equations have the solution

$$\begin{pmatrix} \kappa \\ l \end{pmatrix} = \alpha\begin{pmatrix} b^{\frac{1}{2}} \\ a^{\frac{1}{2}} \end{pmatrix}\exp\{+(ab)^{\frac{1}{2}}s\} + \beta\begin{pmatrix} b^{\frac{1}{2}} \\ -a^{\frac{1}{2}} \end{pmatrix}\exp\{-(ab)^{\frac{1}{2}}s\}, \tag{29}$$

where

$$t = \int^s \left(l + \frac{\mu}{k^2 + l^2}\right)ds'. \tag{30}$$

The constants α and β are determined by the initial values of (k, l). Except for the very special case $\alpha = 0$, $k^2 + l^2 \to \infty$ as $s \to \infty$ and $s \to \infty$ coincides with $t \to \infty$. The vorticity amplitude $(k^2 + l^2)\phi$ is constant in this process. Thus, if an initial localized field $\phi(x, y)$ is Fourier transformed, each individual component ultimately cascades into such small scales that it will be dissipated.

6. The role of viscosity

So far it has been assumed without question that viscosity or other dissipation always reduces the total enstrophy. This cannot be strictly correct, as the following paradox demonstrates. Equation (12) shows that any small change $\delta\psi$ whatever from the flow field ψ_0 results in changes δQ and δE in enstrophy and energy which are of opposite sign. Thus a reduction in enstrophy must be associated with an *increase* in energy. How then does a minimum-enstrophy flow field ψ_0 decay?

In the presence of a slight viscosity ν equation (1) may be written as

$$D(\nabla^2\psi + h)/Dt = \nu\nabla^2(\nabla^2\psi), \tag{31}$$

so that

$$\partial Q/\partial t = \nu\int q\nabla^2(q - h)\,dS$$
$$= -\nu\int \nabla q \cdot \nabla(q - h)\,dS. \tag{32}$$

Thus, only if the dissipation is concentrated in scales for which $h \ll q$ does Q necessarily diminish with time. If ν is small this condition is certainly satisfied in all but the very last stages of the cascade into ψ_0, but for the flow field ψ_0 itself $\partial Q/\partial t$ is slightly positive. The experiments described later do indeed show a large, rapid decrease of Q followed by a slight, slow increase in the final stages.

7. Closed-basin solution

Another point requiring attention is the influence of boundaries. We consider the flow in a closed square basin S with a boundary Γ at which

$$\psi = 0 \tag{33}$$

but with no local restriction on the tangential velocity $\partial\psi/\partial n$. This inviscid
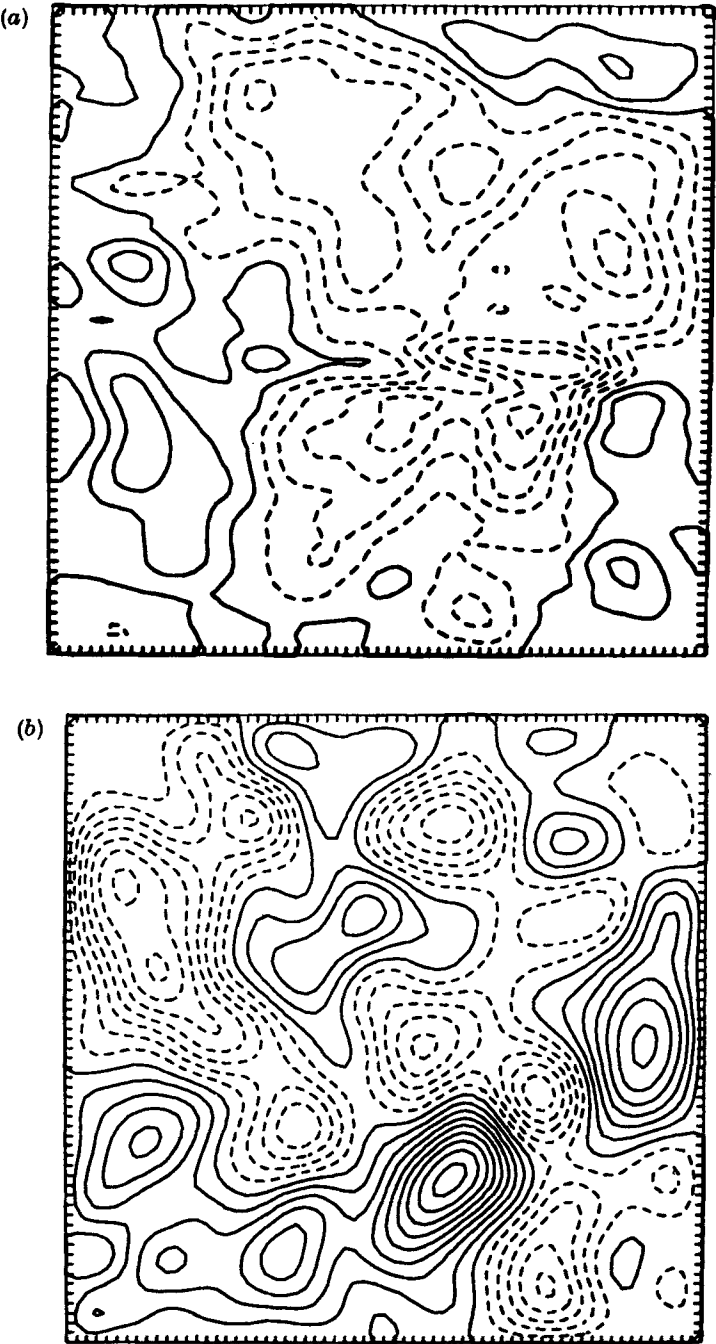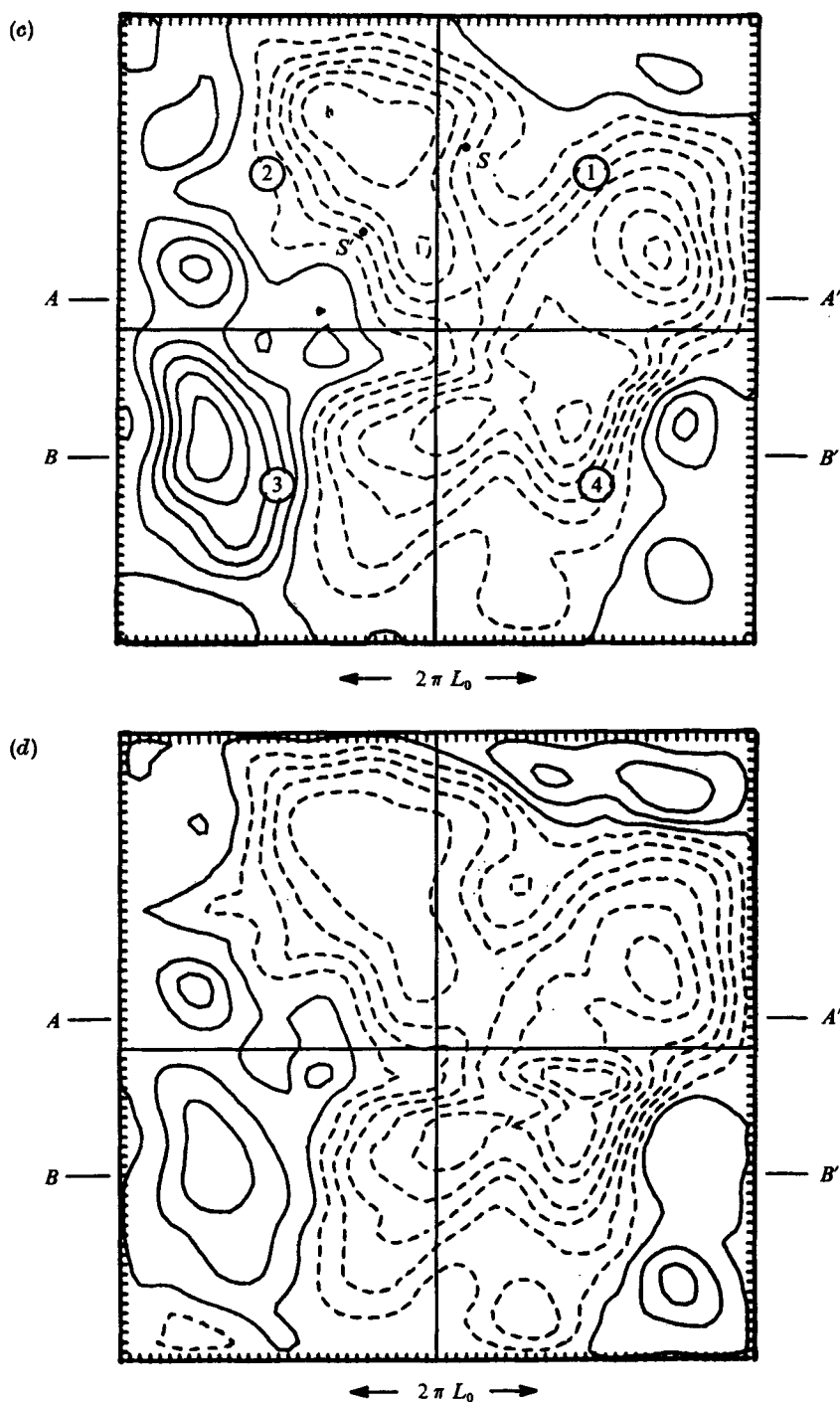
FIGURES 2(*a*, *b*). For legend see next page.

FIGURE 2. Experiment 1. (a) Topography. (b) Initial stream function. (c) Final stream function. (d) Final potential vorticity. Negative contours are broken curves, positive contours are solid. In (c) the circled numbers label the four quadrants; sections along AA' and BB' are shown in figure 4.

condition is, however, not quite adequate because the total circulation

$$C = \int_\Gamma \frac{\partial \psi}{\partial n} ds \qquad (34)$$

is then a constant of the motion and must be treated as given *a priori* when computing the minimum-enstrophy condition. For arbitrary variations satisfying $\psi = 0$ on Γ we require

$$\delta \int_S \tfrac{1}{2}(\nabla^2\psi + h)^2 dS + \mu\delta \int_S |\nabla\psi|^2 dS + \lambda \int_\Gamma \frac{\partial}{\partial n}(\delta\psi) ds = 0. \qquad (35)$$

After several integrations by parts this yields

$$\nabla^2\{\nabla^2\psi + h - \mu\psi\} = 0 \quad \text{within } S \qquad (36)$$

and

$$\nabla^2\psi + h + \lambda = 0 \quad \text{on } \Gamma. \qquad (37)$$

Thus, using (33)

$$\nabla^2\psi - \mu\psi = -(h + \lambda) \quad \text{within } S. \qquad (38)$$

The additional parameter λ is determined by the requirement (34) that the integral of $\nabla^2\psi$ over the whole area should equal C.

Given the boundary condition $\psi = 0$, (38) may be readily treated by half-range Fourier series, and the solution is formally identical to (14), except that the wavenumbers (k, l) are differently quantized.

8. A numerical experiment

We now describe a numerical simulation designed to test the ideas put forward above. The experiments were carried out in a square domain with $\psi = 0$ on the boundary, with a pseudo-spectral model based on a 64×64 half-range sine series as the horizontal expansion. To concentrate the dissipation at the highest possible wavenumbers consistent with the model resolution a fourth-order frictional mechanism was used instead of a regular viscosity, i.e. the right-hand side of (31) was replaced by

$$-\nu'\nabla^4(\nabla^2\psi),$$

implying a corresponding change in (32) to

$$\partial Q/\partial t = -\nu' \int \nabla^2 q \nabla^2(q - h) dS.$$

This formulation is consistent with a slip condition at the boundary Γ, though the circulation around Γ is not strictly constant. However, since the only transfer of vorticity across Γ is diffusive, the circulation just outside a narrow boundary layer, which is the integral of the vorticity over the whole interior, should indeed be independent of time. The coefficient ν' was chosen to give a spin-down time at the wavenumber (16, 16) comparable to the expected relaxation time $4\pi L_0/U$ of the flow field into the steady state. Smaller wavenumbers are scarcely damped at all, but over the next two octaves up to the limit of resolution at the wavenumber (64, 64) the damping rate increases very rapidly, as κ^4. The nonlinear terms in (1) were calculated using pseudo-spectral analogues of the well-known Arakawa (1966) conservative schemes. Besides assuring conservation of energy
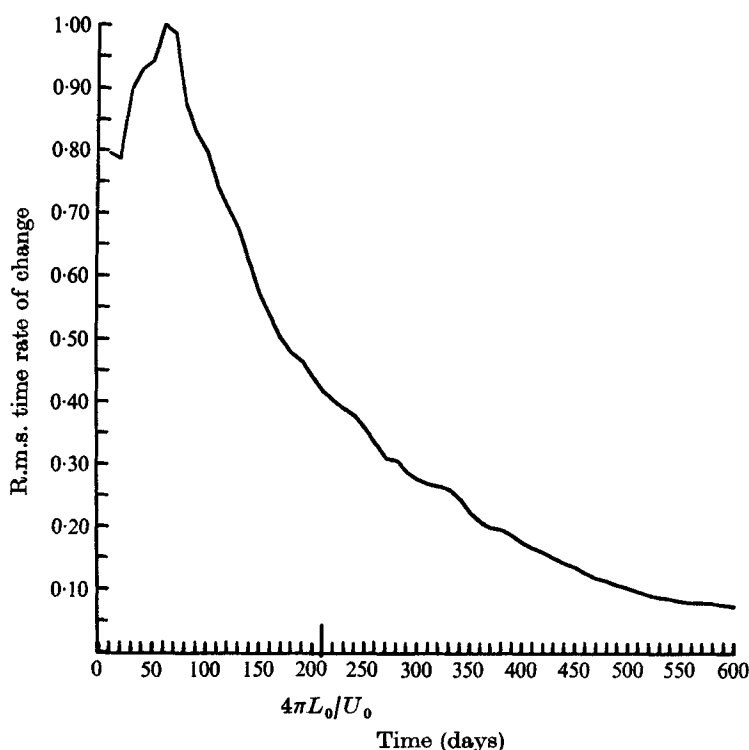
FIGURE 3. $\overline{\{[\partial(\nabla^2\psi)/\partial t]^2\}}^{\frac{1}{2}}$ averaged over the basin as a function of time. The eddy turnover time $4\pi L_0/U_0$ is approximately 210 days.

and enstrophy (apart from dissipation), this formulation is formally of 'infinite' order in the usual spectral sense (Orszag 1971). Stepping forward in time was accomplished by the Lorenz (1971) N-cycle method with $N = 4$ in experiments 1 and 2 and $N = 2$ in experiment 3.

The topography $h(x, y)$ used in experiment 1 is shown in figure 2 (*a*). The initial stream function, shown in figure 2 (*b*), developed into a very nearly steady state, represented by figure 2 (*c*) and its associated potential-vorticity field, figure 2 (*d*). During this 600 day period the total energy dropped by 58 %. Figure 3 shows the root mean square of $\partial q/\partial t$, probably the most sensitive indicator of residual unsteadiness. In fact the major flow features were already set by day 200. In the final state the parallelism of contours of ψ and q is immediately apparent, verifying (21). The linearity of the function $F(\psi)$ is illustrated in figure 4 from sections along the lines AA' and BB' marked in figures 2 (*c*) and (*d*). It is clear that there is strong qualitative agreement with the minimum-enstrophy solution ψ_0 of (13), but there are some significant differences. For example, in the closed anticyclonic gyre near B, $F(\psi)$ is still approximately linear but has only two-thirds of the value appropriate in the central cyclonic eddy which dominates the pattern. Another view is provided by the scatter diagrams in figures 5 (*a*) and (*b*) for the lower two quadrants of the flow field. The solid 45° line corresponds to the least-squares best fit
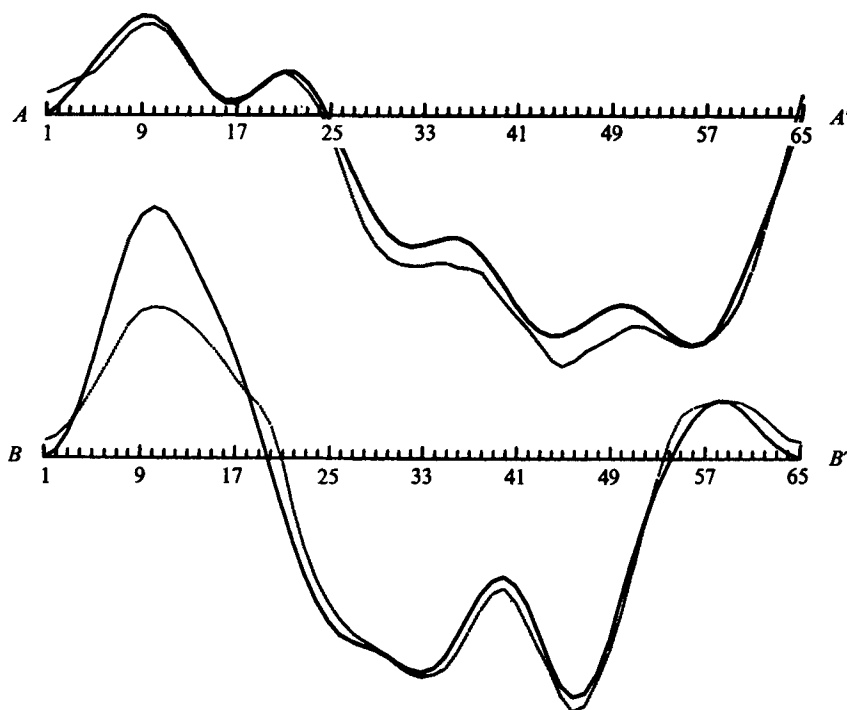
$$q = \mu\psi \tag{39}$$

F. P. Bretherton and D. B. Haidvogel

FIGURE 4. The stream function ψ (solid curves) and potential vorticity q (dotted curves) along sections AA' and BB' in figures 2(c) and (d).

for the field as a whole. The deviations in the gyre near B show up as the cloud of points below the line on the positive side of the origin in quadrant 3. However, the corresponding diagram for quadrant 4 shows deviations in the opposite sense, associated with the gyre in the bottom right-hand corner. Thus to a reasonably accurate approximation the steady state attained in this simulation is identical to that of the minimum-enstrophy solution defined by (14), with the proviso that the value of μ may differ in each of the major closed eddies by a factor as large as 2.

Two further checks on the theory were made. Figure 6 shows the one-dimensional spectrum of the north–south slope $\partial h/\partial y$ averaged over the east–west co-ordinate, together with the corresponding spectra for the east–west component of velocity $-\partial\psi/\partial y$ at day 600 and for the minimum-enstrophy solution computed from (14). For the latter μ was taken from (39) with $\lambda = 0$. $L_0^{-1} = \mu^{\frac{1}{4}}$ corresponds to a wavenumber of 12·9 in the model. (Because of the choice of basis functions, a wavenumber of 1 implies a wavelength *twice* the width of the area shown in figures 2 (a–d).) It is noteworthy how averaging over the lateral co-ordinate to obtain one-dimensional spectra leads to systematic differences in shape between those for slope and velocity, even at length scales substantially greater than L_0. The agreement between spectra for $\partial\psi/\partial y$ and $\partial\psi_0/\partial y$ is remarkably good.

On the other hand, visual inspection of successive plots of potential vorticity yielded no convincing evidence for the role of saddle points of ψ_0 as traps for transient potential-vorticity fluctuations of ever decreasing scale. Nevertheless
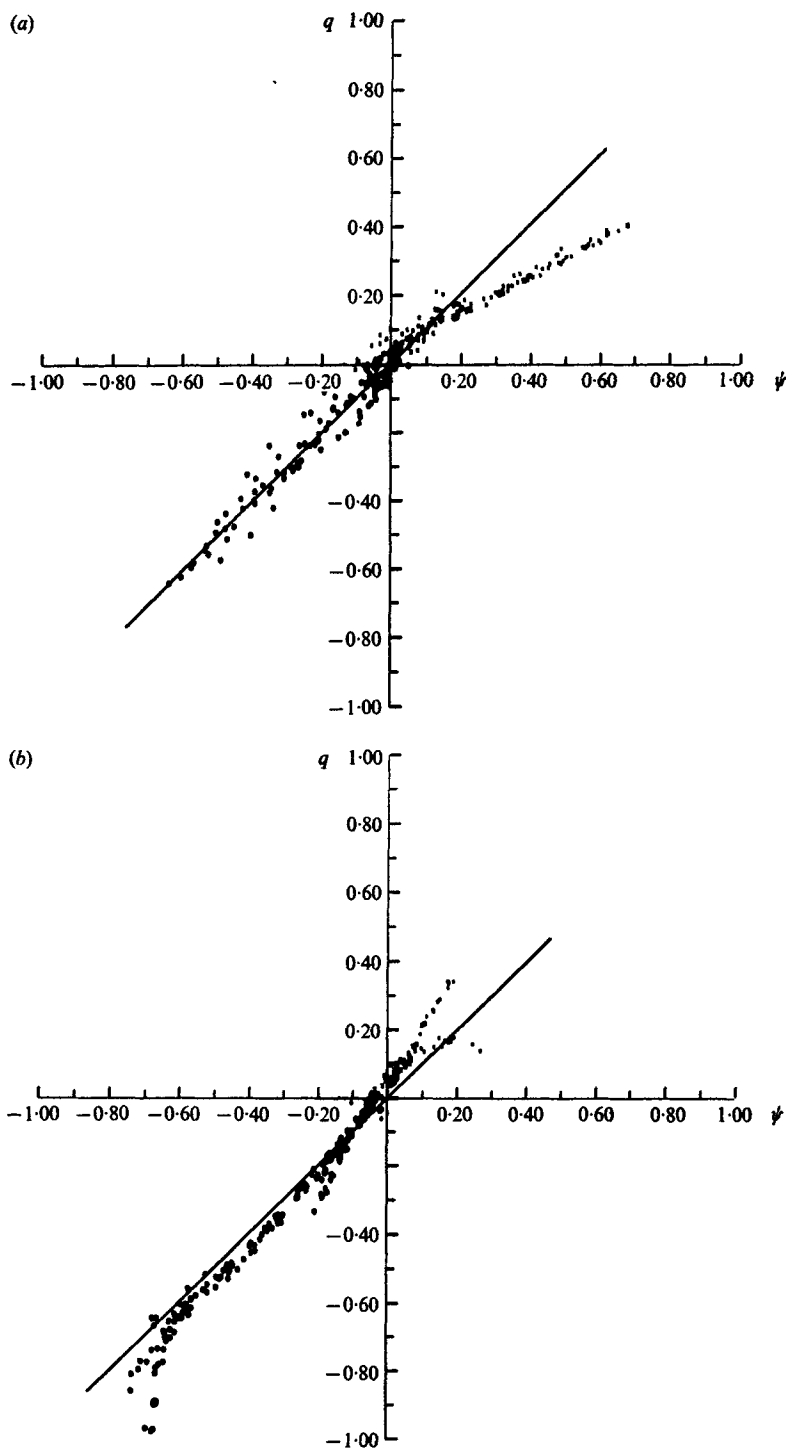
FIGURE 5. Scatter diagrams for potential vorticity *vs.* stream function for (*a*) quadrant 3 and (*b*) quadrant 4, defined in figure 2. The 45° line is the regression line for all quadrants combined.
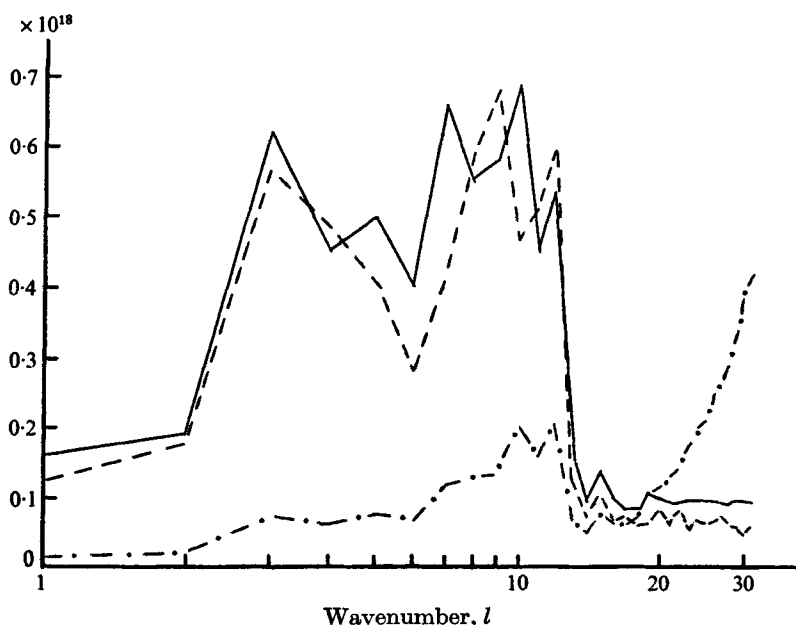
FIGURE 6. One-dimensional spectra for the final state in experiment 1 vs. north–south wavenumber. Ordinates: —·—·—, slope spectrum, $10^6 l^3 \Sigma_k |\hat{h}_{kl}|^2$; ————, velocity spectrum predicted from (14), $l^3 \Sigma_k |\hat{h}_{kl}|^2/(\mu+k^2)^2$; – – –, computed velocity spectrum, $l^3 \Sigma_k |\hat{\psi}_{kl}|^2$. Equal areas beneath the curves correspond to equal contributions to the variance.

figure 7 shows the r.m.s. value of $\partial q/\partial t$ averaged over days 300–600, i.e. over the last part only of the flow development. It will be seen that the transient activity was mainly confined to a band extending around half the periphery of the central gyre in figure 2(c) with an additional centre just upstream of the stagnation point close to A. During the period under consideration a particle initially at point S would have moved to point S'. Very little activity appears to pass the diffluent zone at the bottom right of quadrant 3. Thus the evidence for the suggested trapping mechanism in the later stages of the enstrophy cascade is ambiguous.

Finally, we make some comments on space and time scales. The experimental unit of one day is purely nominal, without significance except in association with scales for h and velocity. For the final state $\psi(x,y)$, the best-fit coefficient in (39) defines a length scale $L_0 = \mu^{-\frac{1}{2}}$. The corresponding wavelength $2\pi L_0$ is indicated in figures 2(c) and (d) and does indeed appear to be a minimum scale for distinguishable features. From the final r.m.s. speed U we have a time scale

$$T_0 = L_0/U = 16 \cdot 9 \text{ days.}$$

However, in two-dimensional turbulence without topography it is the eddy turnover period which is the e-folding time for the enstrophy or the shape of the velocity spectrum. This is roughly $4\pi L/U$, where L is the dominant length scale, corresponding in figure 2(b) roughly to a wavenumber of 6, or about $2L_0$. Thus, allowing for the larger initial value of U a more relevant comparison interval is 300 days. For the parameters used the dissipation at scale L_0 is quite significant

FIGURE 7. $\{\overline{[\partial(\nabla^2\psi)/\partial t]^2}\}^{\frac{1}{2}}$ as a function of position, averaged over days 300–600.

over this interval, so it is perhaps not surprising that about half the initial energy was also lost during the active enstrophy cascade. Presumably, given a much higher spatial resolution and a correspondingly smaller dissipation constant, this would not have occurred.

9. The effects of β

Now consider the addition of a large-scale slope $h = \beta y$ to the random topography considered earlier. In deference to geophysical applications y will be assumed to increase towards the north, and β to be positive. We suppose first that the cascade proceeds essentially as before, and recompute the minimum-enstrophy solution for given total energy E. In so far as the β-slope can be thought of as a Fourier component of zero wavenumber the solution may be instantly obtained:

$$\psi(x, y) = \sum_{k, l} \frac{\hat{h}}{\kappa^2 + \mu} + \frac{\beta}{\mu} y. \tag{40}$$

Thus the effect is to add a large-scale flow of magnitude β/μ from the east. The sign follows from positive β being equivalent to a shallower layer towards the north. If this feature were local, the minimum-enstrophy flow around it would be anticyclonic, i.e. from the east. The total potential vorticity is again constant along the revised streamlines, but there is no provision for the flow to return.

In a closed basin, however, this cannot be. Therefore the influence of boundaries must be non-trivial. It is now the total potential vorticity
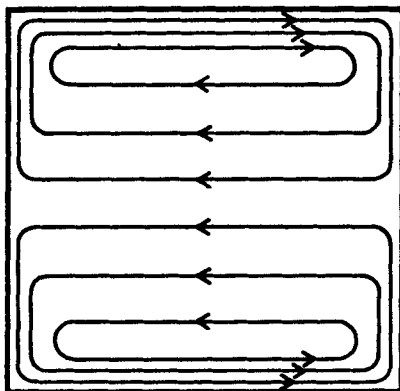
$$q = \nabla^2\psi + h + \beta y \tag{41}$$

FIGURE 8. Schematic stream function for the Fofonoff solution.

which is constant on fluid particles, but the only difference to (35)–(38) is the addition of a term ψ' which satisfies

$$\nabla^2 \psi' - \mu \psi' = -\beta y \quad \text{within } S$$

with
$$\psi' = 0 \quad \text{on } \Gamma. \tag{42}$$

The formal solution in half-range Fourier series proceeds as before, but in the important case when $L_0 = \mu^{-\frac{1}{2}}$ is much less than the dimensions of the basin S a boundary-layer description is more informative. This shows (figure 8) an easterly current

$$\psi' = (\beta/\mu) y$$

throughout the interior, but a narrow return flow in boundary layers of width $\mu^{-\frac{1}{2}}$ all around Γ. These solutions ψ' and associated boundary currents were first described by Fofonoff (1954) as a model for the circulation in the ocean, but they are revealed here as an integral part of the minimum-enstrophy state associated with flow above irregular topography on a β-plane. How far they will in fact be set up depends on the extent of the enstrophy cascade by the small-scale eddies over the interior region!

10. Experiments 2 and 3

To investigate this striking prediction only a simple modification of the previous experiment is required. The dimensionless parameter $K = S_0/\beta$ is a measure of the typical slope of the random topography smoothed to a scale L_0 relative to the large-scale slope equivalent to β. When $K \gg 1$ there are a large number of closed contours of $h + \beta y$. When $K \ll 1$ the contours are all open, describing small perturbations from a uniform gradient. Figure 9 shows the contours for experiments 2 and 3, for which $K = 2$. This value was chosen because it was anticipated that for smaller K the flow would probably resemble linear Rossby waves, for which the enstrophy cascade is very weak, whereas for larger K it would differ too little from that for $K = \infty$, which corresponds to experiment 1.
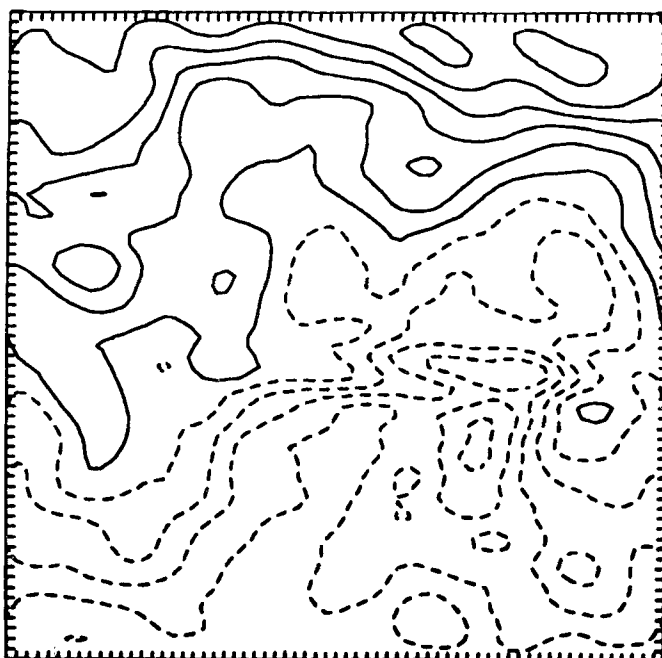
FIGURE 9. Initial topography with beta for experiment 3.

Accordingly, apart from this addition of the Fourier sine series corresponding to βy, the initial conditions for experiment 2 were identical to those described previously. The results were a disaster! No large-scale flow developed: instead the pattern degenerated into a few stationary small-scale isolated eddies which dissipated rapidly, the total energy E falling three times as fast as in experiment 1. The reasons for this behaviour are not completely understood, but it is important because it highlights the limitations of the minimum-enstrophy arguments. In any real experiment at finite Reynolds number some energy dissipation will always occur, but is it slow enough relative to enstrophy dissipation for the qualitative features of the quasi-steady minimum-enstrophy flow to appear? If so the previous discussion is all relevant. Nevertheless, there is no *a priori* reason why energy and enstrophy should not cascade simultaneously to high wavenumbers if the flow structure adjusts itself appropriately, and apparently that is what happened in experiment 2.

In experiment 3 the initial velocities were increased by a factor of 4, and the initial stream function was rotated by $\frac{1}{2}\pi$ relative to the topography. The dissipation coefficient was left unchanged. The stream function and potential vorticity after 500 days are shown in figures 10 (a) and (b).

Several features are immediately apparent. The interior flow shows an easterly trend, with the return along the southern boundary and to a lesser extent along the north. The parallelism between ψ and q is present, but is not as 'clean' as in experiment 1, indicating residual transient disturbances, which appear to be linear oscillations. The functional form of the dependence of q on ψ departs substantially from linear, most of the changes in q being concentrated in only two
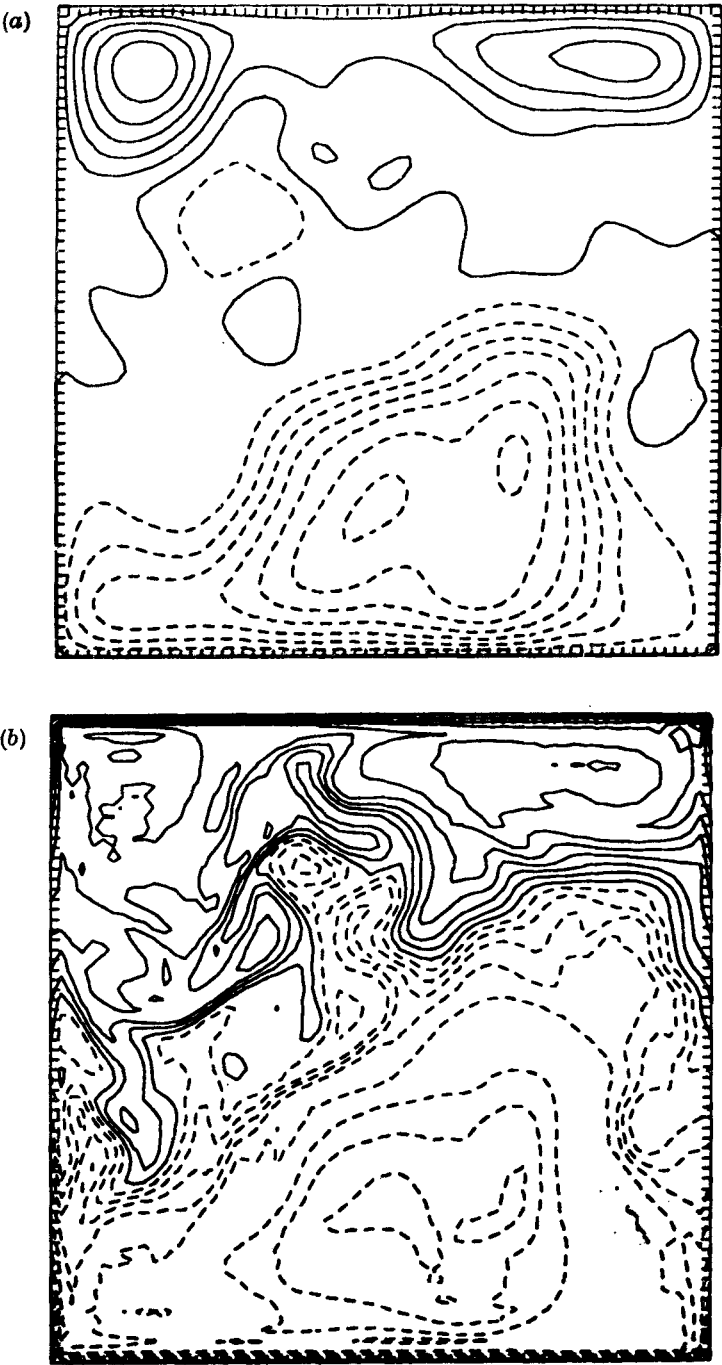
FIGURE 10. Experiment 3. (*a*) Final stream function. (*b*) Final potential vorticity. Broken curves are negative contours.
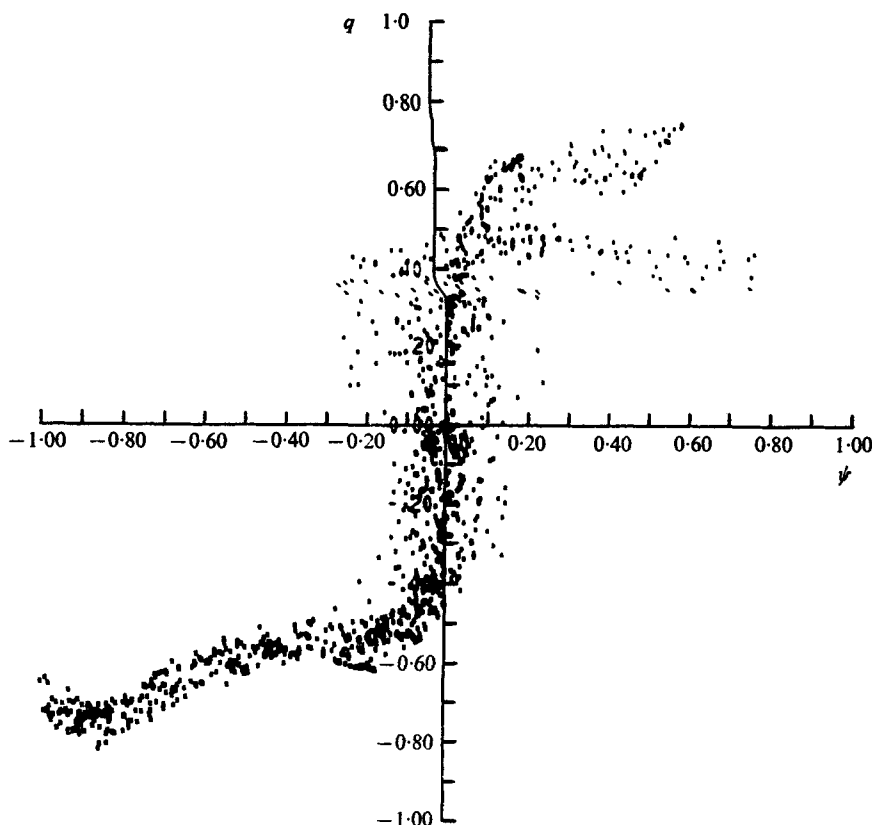
FIGURE 11. Scatter diagram for potential vorticity *vs.* stream function for the entire domain of experiment 3 (see figure 10).

contour intervals for ψ. This is confirmed by the S-shaped appearance of the scatter diagram (figure 11). The scale L_0 determined by a least-squares fit to a straight line is nearly twice the previous value but only 23 % of the sixteen-fold initial kinetic energy was lost in these 500 days. Thus the adjustment time scale

$$T_0 = L_0/U_0 = 6\cdot1 \text{ days}$$

is much less than before and in dynamical terms the integration period is longer by a factor of 2·2. The reasons for the greater persistence of the transients are not clear, although it may possibly be due to the absence of major saddle points.

We conclude that this experiment did confirm qualitatively the predictions of the enstrophy-cascade arguments, though the final state departs more drastically from the minimum-enstrophy solution than in experiment 1. In particular it shows the generally easterly flow parallel to contours of $h + \beta y$, together with the associated boundary layers, but the details are less clear cut than in experiment 1.

11. The effect of eddies on a large-scale flow

To complete this discussion we need to understand how the Fofonoff solution could be driven by small-scale turbulence on the scale of the random topography, and to recognize the transfer process between the large-scale potential vorticity βy and the diffusive enstrophy cascade. The topography plays a crucial role in this transfer. We are concentrating on the transition period while the flow retains its turbulent character. For this purpose we divide the stream function and potential vorticity into 'large-scale' and 'small-scale' parts:

$$\psi = \Psi + \psi', \quad q = (\nabla^2\Psi + \beta y) + (\nabla^2\psi' + h), \tag{43}$$

where ψ' is assumed to be random with zero mean $\overline{\psi'}$. The ensemble average denoted by the overbar is most usefully associated with random realizations of the topography $h(x, y)$, but in some circumstances may be equated with the spatial average over an area large compared with the individual eddies but small compared with the scale for Ψ. It may certainly *not* be considered a time average for given $h(x, y)$. Equation (1) may then be separated into a large-scale part

$$\partial(\nabla^2\Psi)/\partial t + J(\Psi, \nabla^2\Psi) + \beta\Psi_x = -\overline{J(\psi', q')} \tag{44}$$

and an eddy part

$$\partial q'/\partial t + J(\Psi + \psi', q') + J(\psi', \nabla^2\Psi + \beta y) - \overline{J(\psi', q')} = 0. \tag{45}$$

A separation of this sort was implicit in the numerical experiments described by Bretherton & Karweit (1975), which modelled the mesoscale eddies in the ocean. There the large-scale flow was modelled by a uniform stream

$$-\partial\Psi/\partial y = U, \quad \partial Q/\partial y = \beta \tag{46}$$

so the eddy equation became

$$\partial q'/\partial t + U\partial q'/\partial x + J(\psi', q') + \beta\psi'_x = 0. \tag{47}$$

The periodic condition assumed for ψ' and q' implies automatically that $\overline{J(\psi', q')}$ vanishes, and no area average of $\partial q'/\partial t$ over a square of side X can arise.

Whereas this seems a plausible separation when considering the small-scale eddies themselves, a different perspective is necessary when describing their effects on the large-scale flow. The right-hand side of (44) may be written as

$$-\overline{J(\psi', q')} = -\nabla \cdot \mathbf{F}, \tag{48}$$

where $\mathbf{F} \equiv \overline{\mathbf{u}'q'}$ is the local flux of eddy enstrophy. In a statistically homogeneous situation $\mathbf{F}$ may be non-zero but is independent of position. In a nearly homogeneous flow it may still be a good approximation to model the eddies locally by an equation like (47) with periodic boundary conditions, the large-scale velocity $\mathbf{U}$ being regarded as uniform over the area of integration and as a given function of time. $\mathbf{F}$ may then be computed as the area average of $\mathbf{u}'q'$. To the extent that this area average (for one realization $h'(x, y)$) indeed approximates the ensemble average defined above (at a fixed (x, y) but over many realizations h') $\mathbf{F}$ may now

be regarded as a function of position on the *large* scale. Inhomogeneities in the statistics for h' or in the initial eddy energies will imply divergences of F and thus changes in the *large-scale* flow. In any real case this division by scale is clearly an idealization, but presumably is valid asymptotically as spatial inhomogeneities in the eddy statistics become truly slowly varying relative to the dominant scale of the eddies themselves. The estimation of $\mathbf{F}$ in a locally homogeneous small-scale turbulent field then becomes the central problem.

In practice, gradients in large-scale potential vorticity are likely to be dominated by β. Turbulent diffusion in such a gradient inevitably gives rise to eddy fluxes $\mathbf{F}$, but there are several other manifestations of the transfer of large-scale to small-scale enstrophy which deserve to be understood. If

$$q' = \nabla^2 \psi' + h \tag{49}$$

is the eddy enstrophy, (1) may be written as

$$Dq'/Dt = -\beta v' = -\beta \psi'_x. \tag{50}$$

Following a line of reasoning originally begun by Taylor (1921) this may be integrated to give

$$q' = -\beta \eta, \tag{51}$$

where η is the northward displacement from its original position of the particle currently at (x, y). Averaging over the ensemble of particles comprising the turbulent field, and assuming that the latter is statistically homogeneous, the eddy diffusivity may be related by a remarkable series of connexions in turn to the rate of increase of the dispersion of a cloud of marked particles, to the source of eddy enstrophy, to the northward flux of potential vorticity, to the average easterly large-scale body force exerted by the eddies, to the topographic drag associated with pressure differences in the east–west direction across bottom relief, and to the northward virtual mass flux which arises if the bottom relief $h(x, y)$ is replaced by a plane surface. No one of these is a complete description of the particle migration; they are all aspects of the same phenomenon. Thus

$$D = d(\tfrac{1}{2}\overline{\eta^2})/dt = \beta^{-2} d(\tfrac{1}{2}\overline{q'^2})/dt \tag{52a, b}$$

$$= -\beta^{-1} \overline{q'v'} = -\beta^{-1} F^{(y)} = -\beta^{-1} \overline{(\nabla^2 \psi' + h)\, \psi'_x} \tag{52c–e}$$

$$= -\frac{1}{\beta} \left\{ \frac{\partial}{\partial x} \overline{(\psi'^2_x - \psi'^2_y)} + \frac{\partial}{\partial y} \overline{\psi'_x \psi'_y} + \overline{h\psi'_x} \right\} \tag{52f}$$

$$= -\beta^{-1} P^{(x)} = \beta^{-1} M^{(y)}. \tag{52g, h}$$

Most of these steps should be self-explanatory.

Equation (52*f*) clearly describes the divergence of the Reynolds stresses associated with an easterly momentum transfer to the large-scale flow. Now, remembering that h is the true topography times f/H, where H is the total layer depth and f the Coriolis parameter,

$$P^{(x)} = \overline{h\psi'_x} = -\overline{\psi'\, \partial h/\partial x}$$

is $1/\rho H$ times the eastward stress exerted by the container on the fluid through
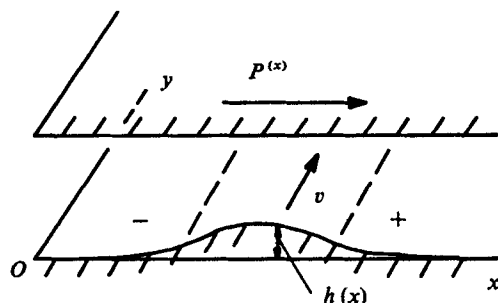
FIGURE 12. The diffusive stress $P^{(x)}$ associated with east–west pressure gradients across topographic features $h(x)$.

pressure differences across topographic features (figure 12). This is usually systematically of one sign, and if large-scale variations take place only over distances large compared with a dominant eddy size, it dominates the first two terms in $(52f)$. Hence the passage from $(52f)$ to $(52g)$ is consistent with our scale separation.

Yet another interpretation arises from considering the changes implied by replacing the lower boundary by the plane surface $h \equiv 0$. If the velocity field $\mathbf{u}' = (-\psi'_y, \psi'_x)$ is extended down to (or truncated at) the new boundary a systematic error will be made in the overall mass flux, the old exceeding the new by the amount

$$\mathbf{M} = -\overline{\mathbf{u}'h}. \tag{53}$$

This is the virtual mass flux which must be added to the flow above a plane surface to parameterize the large-scale effect of the topography h. This interpretation will be taken up later.

Now to see how the small-scale turbulence can set up the circulations associated with the Fofonoff solution, we note that in the interior of the basin the turbulence is indeed associated with a north–south diffusion of fluid particles and a downgradient flux $-\overline{q'v}$ of eddy enstrophy and that the topographic stress P_x is systematically negative, i.e. trying to accelerate the fluid above towards the west. A similar tendency is clearly demonstrated in the multi-level experiments reported by Bretherton & Karweit (1975) and only disappears when a large-scale flow has been generated in response. This fluid returns eastwards in the northern and southern boundary layers. The associated currents display anticyclonic and cyclonic relative vorticity respectively, generated by the enstrophy flux divergence and convergence there required by a southerly flux in the interior yet none through the basin boundaries.

A slightly different interpretation comes from the virtual mass flux $\mathbf{M}$. Suppose for the moment that there is no large-scale flow, i.e. the Eulerian mean velocity is everywhere zero. In the interior there is a southward flux ($F^{(y)} < 0$) of eddy enstrophy, corresponding to a northward virtual volume flux $M^{(y)}$. This means that fluid would be accumulating near the northern boundary. Because this cannot happen there must in fact be a slow southward motion throughout the interior of the fluid, resulting in a large-scale westward acceleration there. However, near the northern boundary, where $M^{(y)}$ is inhibited, the virtual mean

volume flux at the lower boundary is convergent with upward mean motions and horizontal divergence in the fluid above. Thus the mean flow acquires anticyclonic relative vorticity near the northern boundary and sets up the narrow return current of the Fofonoff solution. When the interior westerly velocity has grown sufficiently large, the source of eddy enstrophy ceases, but the small-scale enstrophy cascade continues. Then the flow relaxes into a steady state.

These arguments highlight the importance in this process of eddy-scale topography. In its absence conversion of large-scale to eddy enstrophy is inhibited, because it can be associated only with large-scale gradients of Reynolds stress. Two-dimensional turbulence on a beta-plane above a flat bottom evolves quite differently, into quasi-linear Rossby waves, for which the enstrophy cascade is almost suppressed (Rhines 1975).

Of course, this analysis is an idealization of what actually happened in experiment 3, but it might well be more appropriate if the ratio of basin size to eddy size were increased. This is a matter of model resolution, which is governed primarily by economics. The key concept is of local homogeneity; that is, over a scale large compared with individual eddies yet small compared with the scale of the large-scale flow, spatial averages closely approximate ensemble averages. This is self-consistent only if the dominant contributions to the eddy kinetic energy and to the variance of the slope of the random topography come from smaller scales and a relatively clean separation can be made from the large-scale slope associated with β. The circumstances under which it is relevant to geophysical problems remain to be explored.

12. Conclusions

The enstrophy cascade associated with turbulent eddies in two dimensions implies that the flow will tend to approach a state of minimum enstrophy for a given kinetic energy. For flow above a given topography $h(x, y)$ of random character, this state has steady streamlines, proportional to h on the larger scales but with the finer features smoothed out. The circulation is anticyclonic around shallower regions. Numerical experiment shows that a steady flow resembling this is attained within a few eddy turnover times, though the dependence of the potential vorticity on the stream function is not linear. Deformation fields associated with saddle points in the stream function may act as traps for small perturbations from the steady solution, advecting potential vorticity into very small scales and hastening the reduction to a steady state. A small viscosity tends to dissipate enstrophy on the smallest scales, but can actually increase it on the larger ones, accounting for the ultimate, extremely slow decay of the flow through a sequence of minimum-enstrophy states.

When a large-scale slope corresponding to β is superimposed, the nonlinear evolution depends on the parameter K, which measures the openness of the resultant depth contours. If $K > 1$, the enstrophy cascade proceeds, leading quickly to a steady small-scale flow with a large-scale easterly current superimposed. In a closed basin there is a return flow in narrow boundary layers to the north and south, of a form similar to the Fofonoff model of the ocean circulation.

These predictions are supported qualitatively by numerical experiment. If $K < 1$, on the other hand, quasi-linear Rossby waves dominate and the cascade is greatly slowed. A non-rigorous averaging over the small-scale eddies shows that large-scale flows are driven by the eddy flux of potential vorticity. Determination of this flux should be the goal of any parameterization procedure for the eddies. For spatially homogeneous turbulence on a beta-plane the southward (down-gradient) flux of potential vorticity is related to the particle diffusion coefficient and to conversion of large-scale enstrophy to eddy enstrophy, as well as to a westward stress exerted on the fluid by the topographic features. In a closed basin this stress sets up the easterly flow in the interior region, and qualitatively explains the narrow return boundary layers.

Appendix

This appendix was stimulated by Dr Cecil E. Leith, who drew the attention of the authors to a theorem by Arnold (1965). This states that, in an inviscid fluid, flows with the property that

$$q = F(\psi), \quad dF/d\psi > 0 \tag{A 1}$$

are stable to small disturbances. We here present an extension of Arnold's approach and new results relevant to a slightly viscous fluid with an enstrophy cascade. For simplicity, we consider only an unbounded fluid in which all fields tend to zero at infinity.

Suppose we define a generalized enstrophy integral

$$Q = \int G(q)\, dS, \tag{A 2}$$

where $G(q)$ is any twice differentiable function with positive second derivatives. This has essentially all the properties of the enstrophy defined by (9). For an inviscid non-divergent flow, both q and dS are constant on fluid particles, so Q is a constant of the motion. For a slightly viscous fluid

$$\frac{\partial Q}{\partial t} = \int G'(q) \frac{\partial q}{\partial t} dS$$

$$= \int G'(q) \nu \nabla^2 (\nabla^2 \psi)\, dS$$

$$= \int \nabla \cdot \{\nu G'(q) \nabla(q-h)\}\, dS - \int \nu G''\, \nabla q \cdot \nabla(q-h)\, dS.$$

Now in an unbounded fluid or one with slip boundary conditions the first term vanishes. If also, as in § 6, dissipation is confined to very small scales where $\nabla^2 \psi \gg h$,

$$\frac{\partial Q}{\partial t} = -\int \nu G''(q) |\nabla q|^2\, dS < 0. \tag{A 3}$$

Thus if $G''(q) > 0$, the generalized entropy must decrease with time, and since $G''(q)$ is constant along contours of constant q the cascade process is still just as previously described.

The minimum value of Q for given energy E is given as before by the calculus of variations. For suitable boundary conditions, the condition for a stationery value is

$$G'(q_0) = \mu\psi_0. \tag{A 4}$$

We now show that if $\mu > 0$ the solution to this equation (provided it exists) defines a minimum. Let

$$I \equiv Q + \mu E \tag{A 5}$$

and write

$$\psi = \psi_0 + \phi. \tag{A 6}$$

Expanding in powers of

$$I = I_0 + I_1 + I_2 + O(\phi^3), \tag{A 7}$$

where

$$I_0 = \int\{G(q_0) + \tfrac{1}{2}\mu|\nabla\psi_0|^2\}\,dS, \tag{A 8}$$

I_1 vanishes because (A 4) is satisfied, and

$$I_2 = \tfrac{1}{2}\int\{G''(q_0)\,(\nabla^2\phi) + \mu|\nabla\phi|^2\}\,dS. \tag{A 9}$$

Thus, for positive G'' and μ, I_2 is positive definite, and any slightly perturbed state ψ with the same energy E as ψ_0 must perforce have a larger Q, with equality if and only if $\psi = \psi_0$. Thus $\psi_0(x, y)$ is a unique local minimum. Furthermore, the norm defined by I_2 may be used to infer the existence and good behaviour of neighbouring solutions of (A 4) as μ and the functional form $G(q)$ are varied. It should be noted that (A 4) together with its subsidiary conditions G'', $\mu > 0$ is equivalent to the statement (A 1). Thus for any turbulent realization which settles into a steady flow of this form, we can define *post hoc* the generalized enstrophy $\int G(q)\,dS$ which is minimized in this process. All other measures with $G'' > 0$ decrease under the cascade at the same time, but do not attain their absolute minimum.

Arnold remarked that for an inviscid fluid $Q + \mu E$ is a constant of the motion. Hence if ϕ is small $I_2(\phi)$ must also be constant, and ϕ must remain bounded (according to this norm) for all time. For a viscous fluid dissipating enstrophy but not energy in a cascade this is still true, indeed $||\phi||$ must decrease with time. ψ_0 is thus an absolutely stable state, as indeed are all the other states found by minimizing any permitted measure $Q(q)$. Note that these conclusions fail if the viscosity is so large that the dominant dissipation is on scales for which $\nabla^2\psi$ and h are comparable.

Finally, we make a few remarks about the case when there are extensive regions in the fluid where $G'' < 0$ (assuming still, without loss of generality, that $\mu > 0$). If $G'' = 1$, ψ_0 is readily calculable [e.g. replace μ by $-\mu$ in (14)] and is physically unacceptable. The following comments are not rigorous, but suggest that this behaviour is also typical of the more troublesome nonlinear functions F. Condition (A 4) no longer describes a minimum for G, but a saddle point, and there are problems with both the existence and the uniqueness of ψ_0. The conclusion appears to be that a steady-state flow like (A 1) in which $dq/d\psi < 0$ in substantial regions either does not exist or is likely to be an unstable state which the fluid will not attain in practice.

To show that ψ_0 defines a saddle point, consider a general small perturbation ϕ such that the energy E is unaltered, i.e. satisfying

$$\int\{\nabla\psi_0 \cdot \nabla\phi - \tfrac{1}{2}|\nabla\phi|^2\}\,dS = 0. \tag{A 10}$$

If $|\nabla\phi| \ll |\nabla\psi_0|$, this is a single weak restriction on ϕ, dominated by the first term, and consistent with it we may choose ϕ to be predominantly on a scale L either much less or much greater than $(-G''/\mu)^{\frac{1}{2}}$. In the first case I_2 and $Q-Q_0$ will be negative, in the latter case positive. An initial disturbance of the latter type can disappear with time (so that ψ reverts to ψ_0) only by propagating into regions of the fluid where $G'' > 0$. For if $G'' < 0$, enstrophy cascade and dissipation can only increase $Q-Q_0$ further.

Also if $G'' < 0$ over substantial regions, it is to be expected that

$$G''(q_0)\nabla^2\phi - \mu\phi = 0 \qquad (A\ 11)$$

will have non-trivial solutions $\phi = \phi_0$ which vanish at large distances. Then the solution of (A 4) is clearly non-unique, because any other function of the form $\psi_0 + \alpha\phi_0$, where α is infinitesimal, is also a solution. Also ψ_0 cannot be a continuous function of $G(q)$ or μ. For if we replace G by $G + \delta G$, where δG is infinitesimal, (A 4) becomes

$$G''(q_0)\nabla^2\phi - \mu\phi = -\delta G(q_0). \qquad (A\ 12)$$

The right-hand side of (A 12) is given function of position, and (A 12) has a solution if and only if

$$\int \delta G(q_0)\,\phi_0\,dS = 0, \qquad (A\ 13)$$

a condition which in general will not be satisfied. This application of the familiar Fredholm alternative shows that if $G'' < 0$ not only the uniqueness but also the continuity and perhaps the very existence of solutions of (A 4) are probably lost.

REFERENCES

ARAKAWA, A. 1966 Computational design for long-term numerical integration of the equations of fluid motion: two-dimensional incompressible flow. Part I. *J. Comp. Phys.* **1**, 119–143.

ARNOLD, V. I. 1965 Conditions for nonlinear stability of stationary plane curvilinear flows of an ideal fluid. *Proc. (Dokl.) Acad. Sci. U.S.S.R.* **162**, 773–777.

BATCHELOR, G. K. 1969 Computation of the energy spectrum in homogeneous two-dimensional turbulence. *Phys. Fluids. Suppl.* **12**, II 233–239.

BELL, T. H. 1975 Statistical features of sea-floor topography. *Deep-Sea Res.* **22**, 883–892.

BRETHERTON, F. P. & KARWEIT, M. 1975 Mid-ocean mesoscale modelling. In *Numerical Models of Ocean Circulation*, pp. 237–249. Nat. Acad. Sci.

FOFONOFF, N. P. 1954 Steady flow in a frictionless homogeneous ocean. *J. Mar. Res.* **13**, 254–262.

HERRING, J. R., ORSZAG, S. A., KRAICHNAN, R. H. & FOX, D. G. 1974 Decay of two-dimensional homogeneous turbulence. *J. Fluid Mech.* **66**, 417–444.

HOLLOWAY, G. & HENDERSHOTT, M. 1974 The effect of bottom relief on barotropic eddy fields. *MODE Hot Line News*, no. 65.

LORENZ, E. N. 1971 An *N*-cycle time-differencing scheme for stepwise numerical integration. *Mon. Wea. Rev.* **99**, 644–648.

ORSZAG, S. A. 1971 Numerical simulation of incompressible flows within simple boundaries: accuracy. *J. Fluid Mech.* **49**, 75–112.

RHINES, P. B. 1975 Waves and turbulence on a beta-plane. *J. Fluid Mech.* **69**, 417–443.

TAYLOR, G. I. 1921 Diffusion by continuous movements, *Proc. Lond. Math. Soc.* **20**, 196–212.